COMPDYN 2011
III ECCOMAS Thematic Conference on
Computational Methods in Structural Dynamics and Earthquake Engineering
M. Papadrakakis, M. Fragiadakis, V. Plevris (eds.)
Corfu, Greece, 25–28 May 2011

SEISMIC OVERTURNING OF DAMPED ROCKING STRUCTURES

Elias G. Dimitrakopoulos[1] **and Matthew J. DeJong**[2]

[1] Univeristy of Cambridge, Department of Engineering
Trumpington Street, Cambridge, CB2 1 PZ, UK
ilias.dimitrakopoulos@gmail.com

[2] Univeristy of Cambridge, Department of Engineering
Trumpington Street, Cambridge, CB2 1 PZ, UK
mjd97@cam.ac.uk

Keywords: rocking, overturning, analytical dynamics, earthquake engineering, damping

Abstract. *Numerous structures exhibit rocking behavior during earthquakes and there is a continuing need to retrofit these structures to prevent collapse. The behavior of stand-alone rocking structures has been thoroughly investigated, but there are relatively few theoretical studies on the response of retrofitted rocking structures. In practice, despite the benefits of allowing rocking motion, rocking behavior is typically prevented instead of optimized. This paper characterizes the fundamental behavior of damped rocking motion through analytical modeling. A single rocking block analytical model is utilized to determine the optimal viscous damping characteristics which exploit the beneficial aspects of rocking motion while dissipating energy and preventing overturning collapse. To clarify the benefits of damping, overturning envelopes for the damped rocking block are presented and compared with the pertinent envelopes of the free rocking block. Finally, the same principles of controlling rocking behavior with damping are extended to a particular class of rocking problems, the dynamics of masonry arches. A pilot application of the proposed approach to masonry arches is presented.*

1 INTRODUCTION

Numerous heritage structures exhibit rocking behaviour when loaded dynamically, including monuments, towers, bridge piers, sculptures, etc. Recent earthquakes (e.g. Chile and Italy) have increased world-wide incentive to retrofit such structures to avoid collapse during dynamic loading.

The rocking dynamical response is highly nonlinear and extremely complex; the block displays numerous ways to overturn [1, 2] with respect to the number of the preceding impacts, and its response is highly sensitive on the characteristics of the dynamic loading. Most studies assume an idealized ground excitation in the form of a primary impulse [3] or harmonic loading [1]. The significant amount of research assuming harmonic loading originates from the concept that a constant frequency excitation can cause resonance. However, one main advantage of the rocking system is that constant frequency rocking resonance is impossible because the natural frequency changes with rocking amplitude. Further, harmonic ground motions which could cause rocking resonance would have to have a precise time-varying frequency, and are thus extremely unlikely [4]. Rocking behaviour is mostly affected by the distinct time-dependent characteristics of the ground excitation that are less relevant to the response of elastically deformable structures.

In contrast to the significant amount of research on the response of stand-alone rocking structures, there are only a handful of theoretical studies on the response of retrofitted rocking structures [5, 6]. In practice, rocking behaviour is typically prevented instead of limited or confined. Prevention is achieved by tying structures down, reinforcing them internally by drilling through or externally by wrapping with Fibre-Reinforce Polymers (FRP) [7].

While these methods can be effective, they can over-stiffen structures, add stress, and be destructive. More particular, Makris & Zhang [5] showed that the response of the anchored rocking block can be worse of that of the pertinent stand-alone rocking block. In addition, when earthquake loading is rare and relatively minimal, as in the UK, extensive reinforcing of a vast number of structures may be economically infeasible and too invasive for heritage structures. Hence, application of intelligent less invasive intervention methods is sought, through confinement of the rocking response instead of prevention. This research aims to lay the foundation for the development of a new class of retrofit solutions which exploit damping systems.

2 DAMPED ROCKING MOTION

Motivated by the inverse effects of adding strength to the rocking block, this research takes an alternative approach and investigates the benefits of additional damping. Consider first the free standing rocking block of Figure 1 (without dampers) subjected to a pulse-type base excitation with acceleration amplitude a_g and frequency ω_g. Assuming the coefficient of friction is high enough to prevent sliding, the rocking motion initiates when the ground acceleration $\ddot{u}_g$ exceeds the critical value: $\ddot{u}_g \geq a_{g,\,min} = g\,tan\alpha$ where α is the angle of slenderness and g the gravity acceleration.

The moment equilibrium, during rocking, with respect to the pivot points O (or O' accordingly in Figure 1) gives:

$$I_0\ddot{\theta} + mgR\sin\left[\alpha\,\mathrm{sgn}(\theta) - \theta\right] = -m\ddot{u}_g R\cos\left[\alpha\,\mathrm{sgn}(\theta) - \theta\right] \tag{1}$$

where θ is the rocking rotation, I_0 the moment of inertia with respect to the pivot point, m the mass of the block, R the half-diagonal and $sgn()$ the standard sign function. The slenderness angle is defined by $\tan\alpha = b/h$, where $2b$ is the width and $2h$ the height of the block.

To complete the description of the problem, the equation of motion is complemented with a coefficient of restitution η, defined as the ratio of the pre and post impact velocities, which ranges between 0 (for perfectly plastic) and 1 (for perfectly elastic impact):

$$\dot{\theta}^{+} = \eta \dot{\theta}^{-} \tag{2}$$

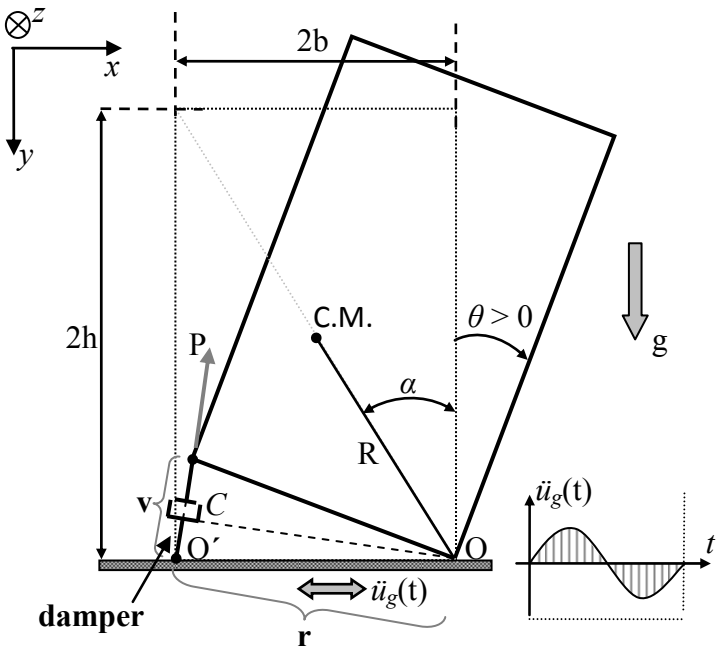

Figure 1: The rocking block retrofitted with viscous dampers at its edges.

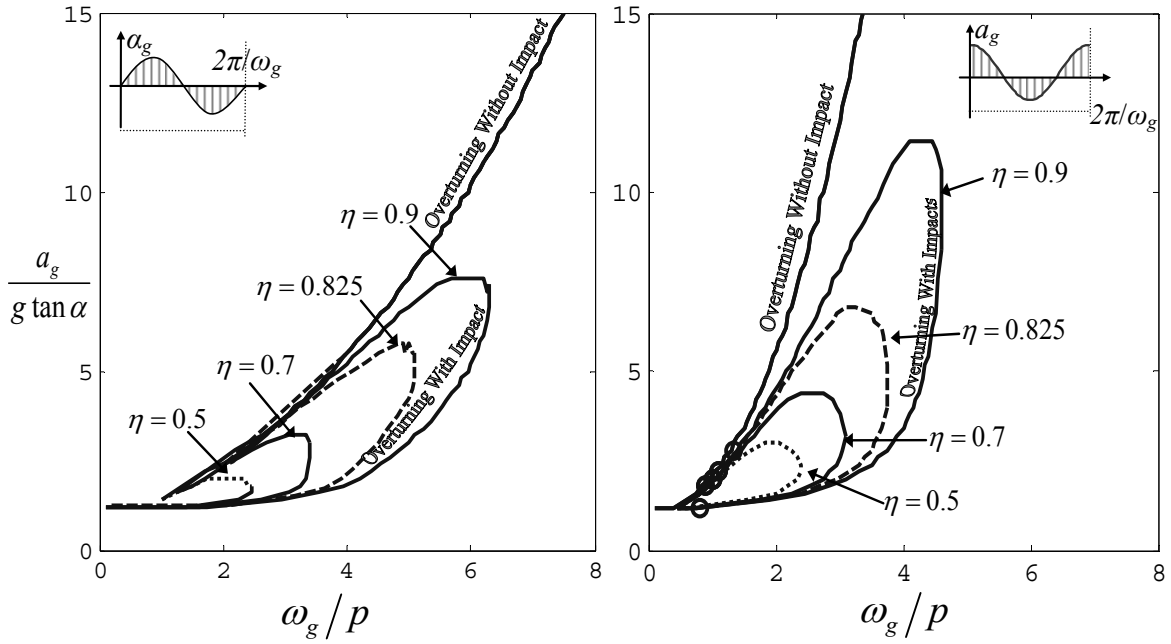

Figure 2: Overturning envelopes of the stand-alone rocking block for different coefficients of restitution η.

The present description of rocking (Equations 1 and 2), is valid under the assumption that the block is slender enough to prevent other impact behaviors to arise such as bouncing.

Figure 2 presents the overturning envelopes of the rocking block, subjected to simple trigonometric pulses, for different coefficients of restitution η. As expected, the coefficient of restitution affects the overturning of the rocking block only when impacts precede overturning. In other words, the energy is damped out of the stand-alone rigid block only during impacts. This poses a theoretical limit to reducing rocking behaviour by increasing energy dissipation at impact, as immediate overturning is unaffected.

2.1 Bilateral Viscous Dampers

As a first approach, consider a rigid block retrofitted with bilateral viscous dampers as in Figure 1. The force P of a viscous linear damper is given by:

$$P = C\dot{v} \tag{3}$$

where $\dot{v}$ is the relative velocity between the ends of the damper and C the damping constant.

Moment equilibrium of the retrofitted block (Figure 1) during rocking gives:

$$I_0\ddot{\theta} + mgR\sin\left[\alpha\,\mathrm{sgn}(\theta) - \theta\right] + P\cdot r = -m\ddot{u}_g R\cos\left[\alpha\,\mathrm{sgn}(\theta) - \theta\right] \tag{4}$$

where r is the lever of the damping force P.

Equation (4) can be written using Eq.(3)and geometric properties:

$$\ddot{\theta} = -p^2\left\{\sin\left[\alpha\,\mathrm{sgn}(\theta) - \theta\right] + \frac{\ddot{u}_g}{g}\cos\left[\alpha\,\mathrm{sgn}(\theta) - \theta\right]\right\} - p\gamma\left(1+\cos\theta\right)\dot{\theta} \tag{5}$$

where $p = \sqrt{3g/4R}$ is the frequency parameter of the block, and $\gamma \doteq \frac{3}{2}\frac{C}{mp}\sin^2\alpha$ is a dimensionless parameter that relates the damping constant C to the mass m, slenderness α and frequency p.

2.2 Unilateral Viscous Dampers

Re-centering, i.e. limiting residual displacements despite large displacement during seismic loading, is an advantage of rocking motion. However, collapse must be prevented. Thus, to limit collapse while encouraging re-centering, unilateral viscous dampers, which are activated only during uplift, are also considered. The behaviour of such unilateral viscous dampers can be described with the help of an ad-hoc function $S\left(\theta,\dot{\theta}\right)$ defined as follows:

$$S\left(\theta,\dot{\theta}\right) = \frac{1}{2}\left[\mathrm{sgn}\left(\theta\cdot\dot{\theta}\right)+1\right] = \begin{cases} 1 \textit{ when uplifting} \\ 0 \textit{ when restoring} \end{cases} \tag{6}$$

The equation of motion for the linear unilateral viscous damper is:

$$\ddot{\theta} = -p^2\left\{\sin\left[\alpha\,\mathrm{sgn}(\theta) - \theta\right] + \frac{\ddot{u}_g}{g}\cos\left[\alpha\,\mathrm{sgn}(\theta) - \theta\right]\right\} - p\gamma\left(1+\cos\theta\right)S\left(\theta,\dot{\theta}\right)\dot{\theta} \tag{7}$$

2.3 Response of the damped rocking block to pulse-type excitations

Figure 3 presents the overturning envelopes for the bilateral damping, and Figure 4 presents the overturning envelopes for the equivalent unilateral (same γ parameter) dampers. Both figures also contain the undamped (stand-alone) rocking block envelopes. The block is excited with simple trigonometric pulses and the response is calculated by numerically solving the nonlinear differential equations of motion (Eq. 5 and 7 respectively) assuming a constant coefficient of restitution η. The behaviour is described in the dimensionless terms:

$$\frac{a_g}{g\tan\alpha},\ \frac{\omega_g}{p},\ \eta,\ \gamma=\frac{3}{2}\frac{C}{mp}\sin^2\alpha \tag{8}$$

Similarly to the behavior of the stand-alone rocking block [3], the damped rocking block displays two different modes of overturning under a sine and a cosine pulse-excitation (e.g. Figure 3): immediate overturning without impact and overturning with at least one impact (one in the case of a sine pulse excitation and up to 2 in the case of a cosine pulse excitation). In genera land as expected, the overturning-with-impact mode is more critical since it appears for lower excitation intensities. However, unlike the case of additional strength [5], the higher the additional damping (parameter γ), the more the overturning envelopes shrink, regardless of the excitation type (sine or cosine).

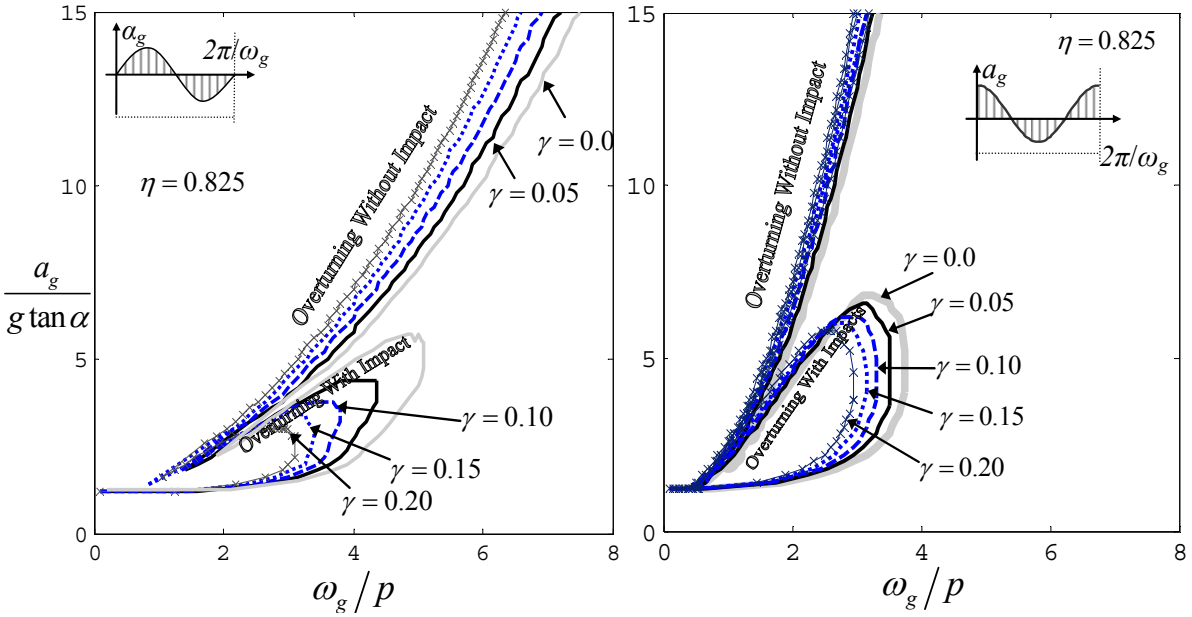

Figure 3: Overturning envelopes for the rocking block with bilateral viscous dampers. Comparison with the stand-alone rocking block (thick grey line).

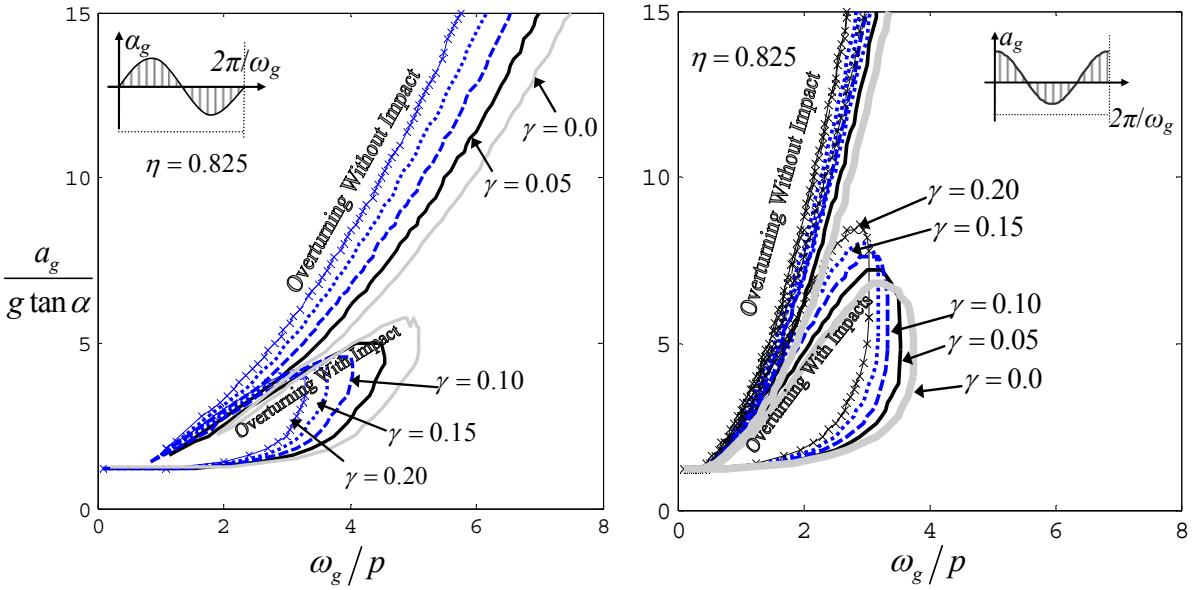

Figure 4: Overturning envelopes for the rocking block with unilateral viscous dampers. Comparison with the stand-alone rocking block (thick grey line).

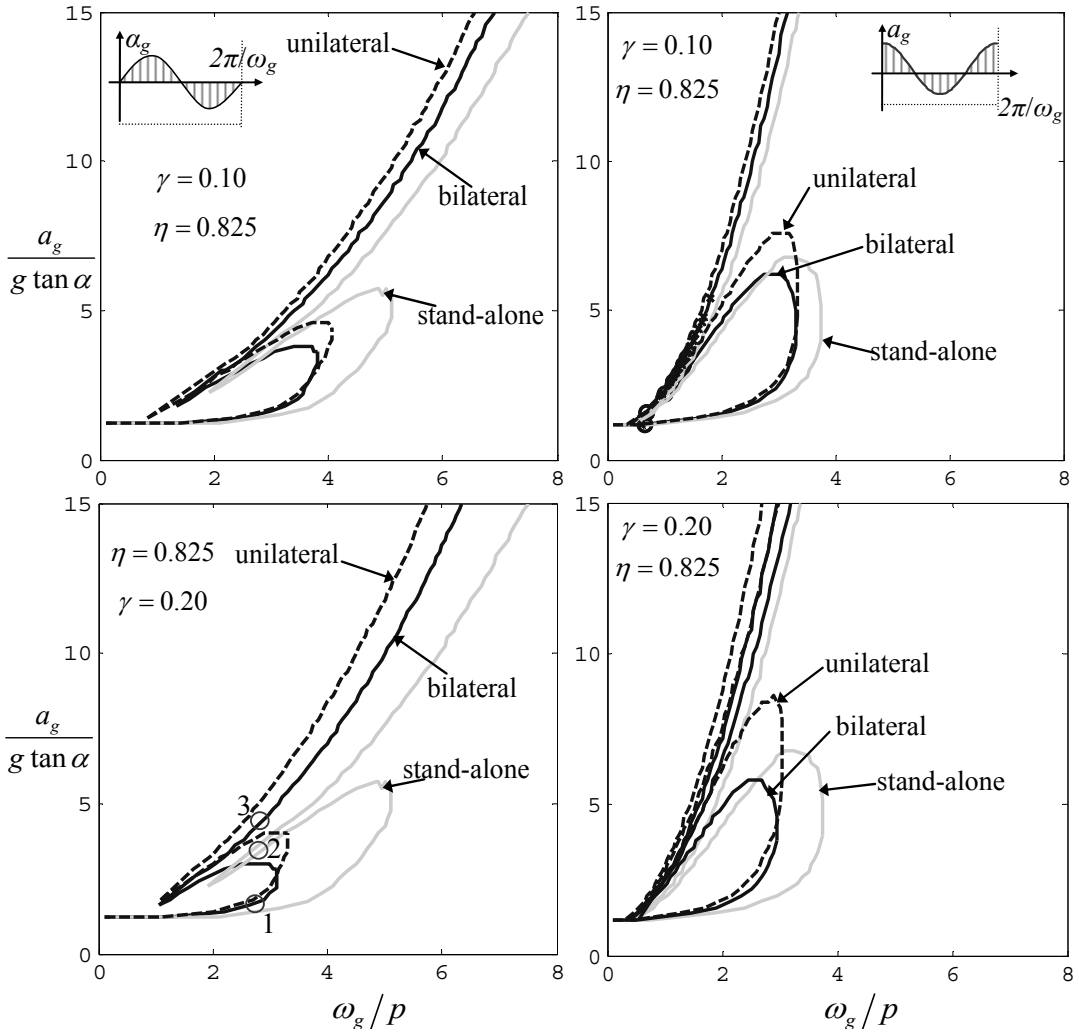

Figure 5: Comparison of overturning envelopes for the rocking block retrofitted with bilateral and unilateral viscous dampers.

In Figure 5, the overturning envelopes for bilateral and unilateral damping are directly compared. Both unilateral and bilateral dampers have a similar beneficial effect for overturning without impact. However, there is a brief change in velocity prior to overturning during which the block tries to recover. Bilateral dampers limit this recovery, while unilateral dampers allow it, making them slightly more effective.

For overturning with impact, both damping options cause a similar beneficial shift in the minimum impulses which cause overturning (the lower limit of the overturning area shifts up and left). However, bilateral dampers provide a larger decrease of the total overturning area through a larger downward shift in the upper limit of the overturning region. While may be beneficial, it should be noted that the intermediate safety area, between the two overturning basins, is a result of the highly nonlinear behavior of the rocking block and is very sensitive to the characteristics of the excitation [1, 2]. Thus, from a design perspective, it is unreliable to depend on this safety region, and the lower limit is more important. Hence, both options have a remarkably similar benefit.

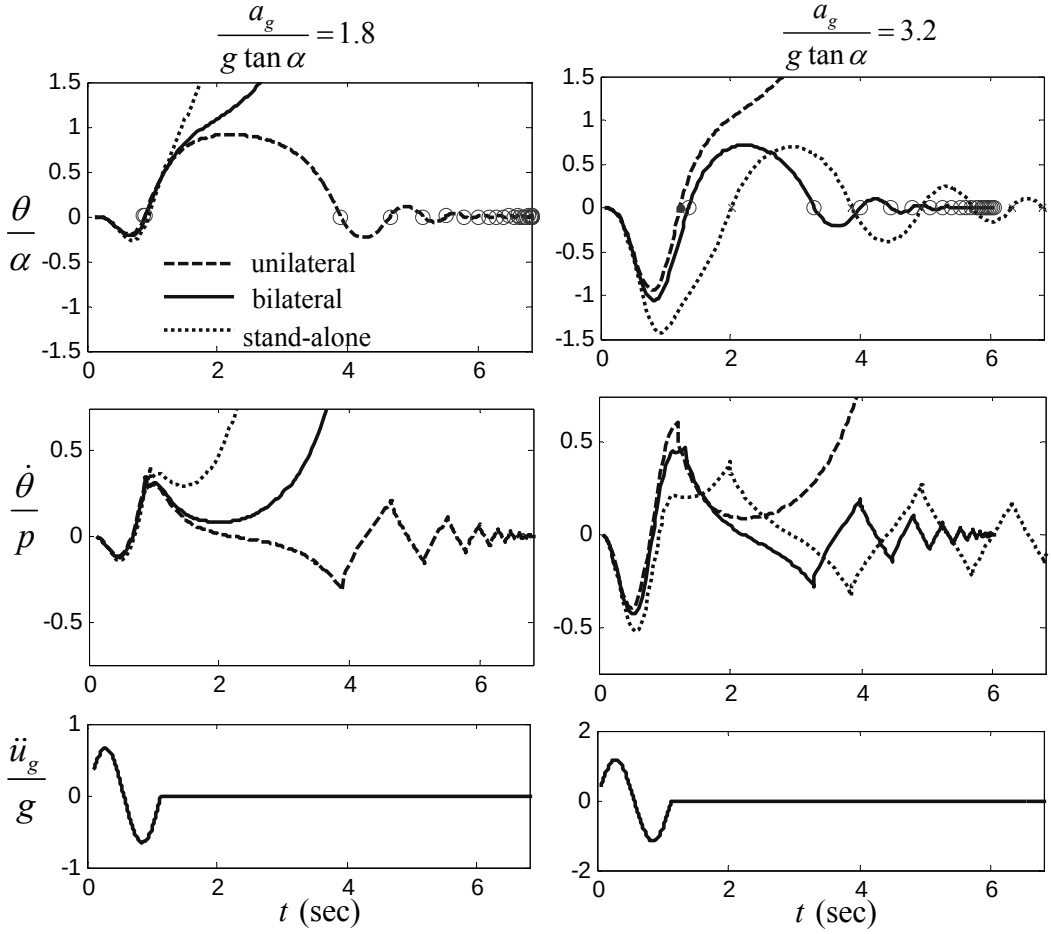

Figure 6: Rocking rotation (top) and angular velocity (middle) time-history of the rocking block ($\omega/p = 2.75$, $\eta = 0.825$) excited with a sine pulse (bottom). Left column point 1 of Figure 5 and right column point 2 of Figure 5.

To further investigate the effects of adding damping and the sensitivity of the rocking response, Figure 6 plots the time-history response (rotation and angular velocity) of the rocking block that corresponds to the points 1 to 3 in the overturning diagram (Figure 5). For $a_g/(g\tan\alpha) = 1.8$ and 4.6 (points 1 and 3) the stand-alone and the bilaterally damped rocking

block overturn, while the unilaterally damper rocking block survives. On the contrary, for $a_g/(g\ \tan\alpha) = 3.2$ (point 2) the opposite is true: the stand-alone and the bilaterally damped block survive, while the unilaterally damped block overturns. The response is clearly highly nonlinear, and numerous instances where either the bilateral or the unilateral damper performs better can be found. As a general rule, for a given damping parameter γ the performance of the two types of damper are comparable.

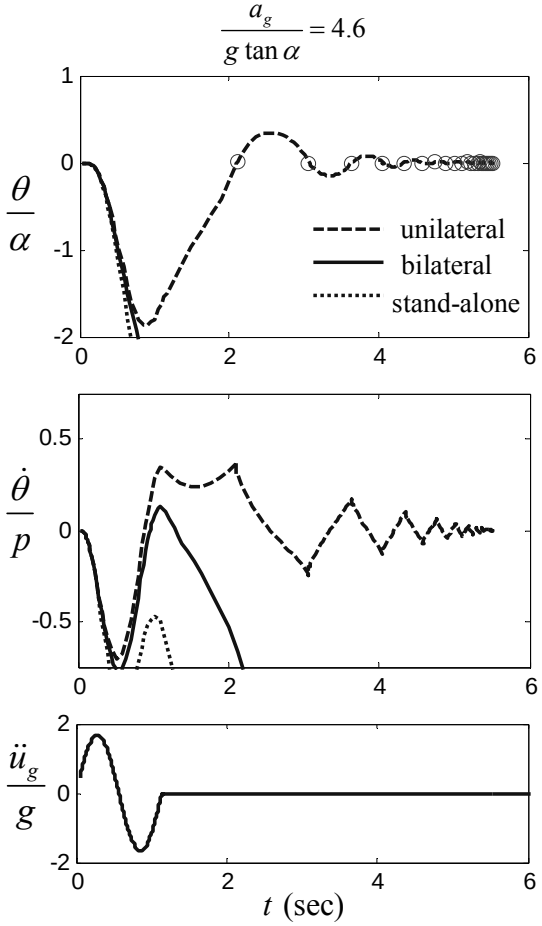

Figure 7: Rocking rotation (top) and angular velocity (middle) time-history of the rocking block ($\omega/p = 2.75$, $\eta = 0.825$) excited with a sine pulse (bottom). Point 3 of Figure 5.

3 DAMPING OF MASONRY ARCH ROCKING

The dynamics of masonry arches is a particular class of rocking problems. Under specific conditions outlined in DeJong et al. [8], Oppenheim [9] and Sinopoli [10], the dynamics of the masonry arch can be captured with a single degree of freedom model (SDOF). For single pulse dominated earthquake motions, an SDOF arch model was effective in predicting experimental collapse results for dry-stone masonry arches [8]. Further, arches are prolific in historic structures which stand vulnerable to seismic loading. Retrofit solutions which incorporate damping could potentially provide a viable solution for improving seismic safety.

As a first approach, the damping formulation presented in section 2 is here extended to masonry arches. It is assumed that linear viscous damping is added at hinging locations in the masonry arch, without considering a specific geometrical damper configuration.

The SDOF equation of motion can be derived from Hamilton's principle and Lagrange's equation:

$$\frac{\partial}{\partial t}\left(\frac{\partial T}{\partial \dot{\theta}}\right)-\frac{\partial T}{\partial \theta}+\frac{\partial V}{\partial \theta}=Q \tag{9}$$

The kinetic energy T and the potential energy V can be found in [9]. The generalized force expression is comprised of two parts: the inertial terms due to base excitation Q_g [9] and the additional damping forces Q_d. The total generalized force becomes $Q = Q_g + Q_d$.

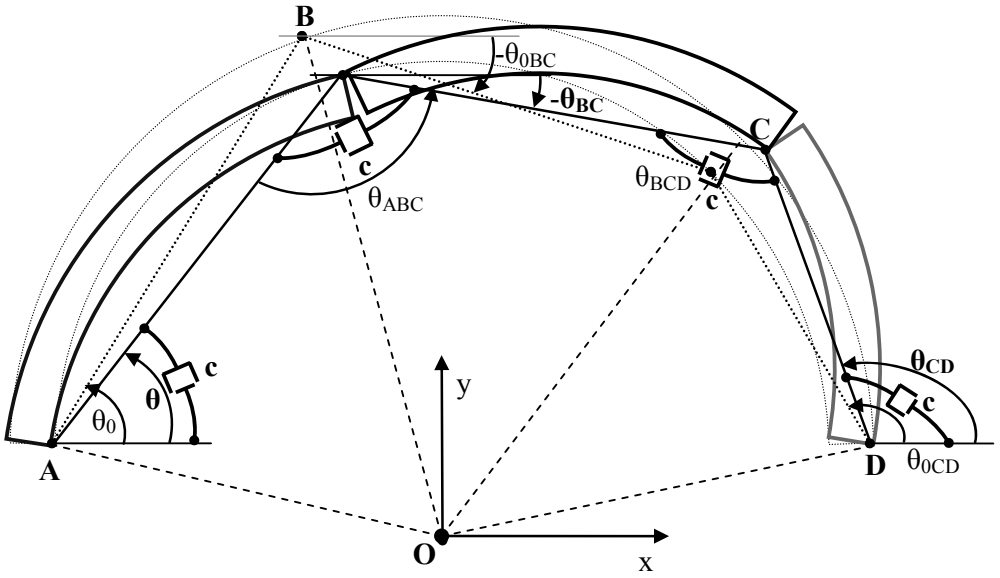

Figure 8: The four-link kinematical mechanism of a masonry arch, during rocking under base excitation. Additional linear viscous damping is assumed at hinging locations.

The damping force Q_d can be determined after calculating the work of the non-conservative forces δW_{nc} as:

$$\delta W_{nc}=Q\delta\theta=\left(Q_g+Q_d\right)\delta\theta \tag{10}$$

In particular:

$$\begin{aligned}
&Q_d\delta\theta=-c\cdot\dot{\theta}\delta\theta-c\cdot\dot{\theta}_{ABC}(\theta)\delta\theta_{ABC}-c\cdot\dot{\theta}_{BCD}(\theta)\delta\theta_{BCD}-c\cdot\dot{\theta}_{CD}(\theta)\delta\theta_{CD}=\\
&Q_d\delta\theta=-c\left[1+\left(\frac{\partial\theta_{BC}}{\partial\theta}(\theta)-1\right)^2+\left(\frac{\partial\theta_{CD}}{\partial\theta}(\theta)-\frac{\partial\theta_{BC}}{\partial\theta}(\theta)\right)^2+\left(\frac{\partial\theta_{CD}}{\partial\theta}(\theta)\right)^2\right]\dot{\theta}(t)\delta\theta\Rightarrow\\
&Q_d=-c\left[1+\left(\frac{\partial\theta_{BC}}{\partial\theta}(\theta)-1\right)^2+\left(\frac{\partial\theta_{CD}}{\partial\theta}(\theta)-\frac{\partial\theta_{BC}}{\partial\theta}(\theta)\right)^2+\left(\frac{\partial\theta_{CD}}{\partial\theta}(\theta)\right)^2\right]\dot{\theta}(t)
\end{aligned} \tag{11}$$

where θ_{AB}, θ_{ABC}, θ_{BCD}, θ_{CD} are the angles depicted in Figure 8, and c is the damping constant. After extensive algebra, the equation of motion can be written in the form:

$$M(\theta)R^3\ddot{\theta}+L(\theta)R^3\dot{\theta}^2+F(\theta)R^2g+D(\theta)R^2\dot{\theta}=P(\theta)R^2\ddot{x}_g \tag{12}$$

where $D(\theta)$ is the term introduced due to damping.

Figure 9 plots the time-history response of the masonry arch described in Oppenheim [9], to a simple sine ground motion with acceleration amplitude $a_g = 0.75\ g$ and duration $T_g = 1.0$ sec (Figure 9 bottom). The coefficient of restitution is taken as $\eta = 0.93$. The free masonry arch fails during rocking, while the addition of (linear) viscous damping at the hinging locations prevents failure.

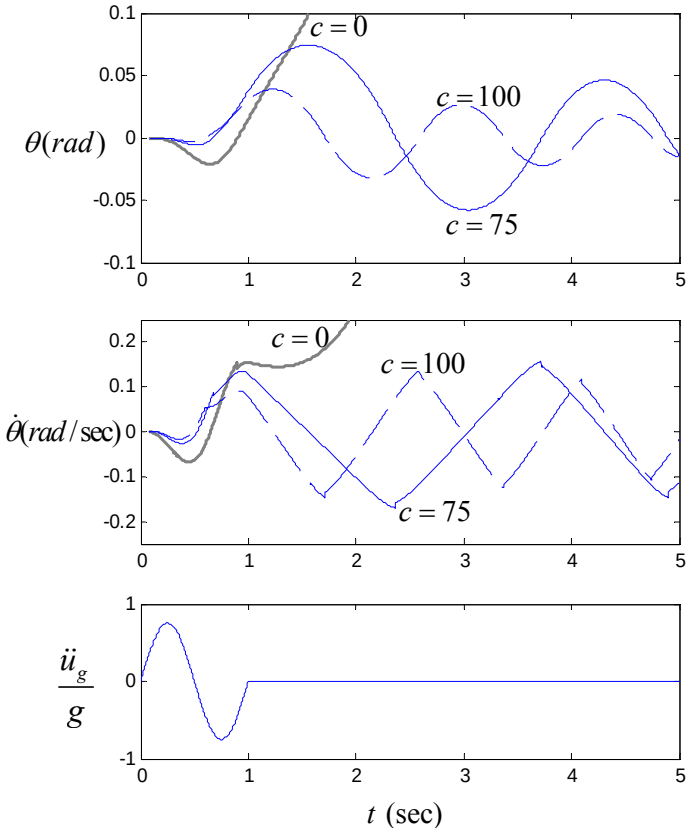

Figure 9: Rocking of the masonry arch under a sine pulse excitation (bottom). Rotation (top) and angular velocity (middle) about left hinge. While the free ($c = 0$) arch fails, the addition of damping ($c = 75$, 100 m sec kN).

4 CONCLUSIONS

In this paper the consequences of adding damping to rocking structures are investigated. Interestingly, while additional damping is already implemented in practice, to retrofit rocking structures, there is a lack of theoretical research on the subject.

The overturning envelopes of a rocking block retrofitted with bilateral and unilateral (activated only during uplift) linear viscous dampers, show a substantial enhancement of the behaviour. As a general rule, for a given damping level, the performance of the two types of damper are comparable. However, the unilateral damper delays the first appearance of overturning with impact and the first appearance of overturning without impact mode, but the area of overturning with impact is larger, compared to the pertinent bilateral damped block. Comparing with the alternative of anchoring the rocking system, the additional damping does not lead to counter effects where the behaviour of the retrofitted rocking system is actually worse than that of the stand-alone system.

The masonry arch exemplifies an alternate type of rocking structure for which added damping might be appropriate.

REFERENCES.

[1] S.J. Hogan. The many steady state responses of a rigid block under harmonic forcing. *Earthquake Engineering Structural Dynamics*, 19(7), 1057-1071, 1990

[2] R.H. Plaut. Fractal Behavior of an Asymmetric Rigid Block Overturning Due to Harmonic Motion of a Tilted Foundation. *Chaos Solitons & Fractals*. 7(2), 177-196, 1995

[3] J. Zhang, N. Makris. Rocking Response of Free-Standing Blocks under Cycloidal Pulses. *Journal Engineering Mechanics*. 127(5), 473, 2001

[4] M.J. DeJong. Seismic Assessment Strategies for Masonry Structures. PhD Thesis, Massachusetts Institute of Technology (MIT), 2009

[5] N. Makris, J. Zhang. Rocking Response of Anchored Blocks under Pulse-Type Motions. *Journal Engineering Mechanics*.127(5), 484, 2001.

[6] A. Di Egidio, A. Contento. Base isolation of slide-rocking non-symmetric rigid blocks under impulsive and seismic excitations. *Engineering Structures*. 31(11), 2723-2734, 2009.

[7] S. Pampanin. Controversial aspects in seismic assessment and retrofit of structures in modern times: understanding and implementing lessons from ancient heritage. *Bulletin of the New Zealand Society for Earthquake Engineering*. 39(2), 120-133, 2006.

[8] M.J. DeJong, L. De Lorenzis, S. Adams, J.A. Ochsendorf. Rocking Stability of Masonry Arches in Seismic Regions. *Earthquake Spectra*. 24(4), 847, 2008.

[9] I.J. Oppenheim. The masonry arch as a four-link mechanism under base motion. *Earthquake Engineering Structural Dynamics*. 21(11), 1005-1017, 1992.

[10] A. Sinopoli. A semi-analytical approach for the dynamics of the stone arch. *Proceedings of the ICE - Engineering and Computational Mechanics,* 63(3), 167-178, 2010.